Available online at www.sciencedirect.com
ScienceDirect
Palaeogeography, Palaeoclimatology, Palaeoecology 246 (2007) 292–306
PALAEO
www.elsevier.com/locate/palaeo

Paleoenvironmental changes in the western Mediterranean since the last glacial maximum: High resolution multiproxy record from the Algero–Balearic basin

Francisco J. Jimenez-Espejo [a,*], Francisca Martinez-Ruiz [a], Tatsuhiko Sakamoto [b], Koichi Iijima [b], David Gallego-Torres [a], Naomi Harada [c]

[a] *Instituto Andaluz de Ciencias de la Tierra, CSIC-Universidad de Granada, Facultad de Ciencias, Avda. Fuentenueva, s/n, 18002 Granada, Spain*
[b] *Institute for Research on Earth Evolution (IFREE), Japan Agency for Marine-Earth Science and Technology (JAMSTEC), 2-15 Natsushima-cho, Yokosuka 237-0061, Japan*
[c] *Institute of Observational Research for Global Change, Japan Agency for Marine-Earth Science and Technology (JAMSTEC), 2-15 Natsushima-cho, Yokosuka 237-0061, Japan*

Received 30 December 2005; received in revised form 10 October 2006; accepted 13 October 2006

Abstract

The present study uses a multiproxy approach in order to further understand the evolution of climate responses in the western Mediterranean as of the Last Glacial Maximum. Sediments from ODP Site 975 in the Algero–Balearic basin have been analysed at high resolution, both geochemically and mineralogicallly. The resulting data have been used as proxies to establish a sedimentary regime, primary marine productivity, the preservation of the proxies and oxygen conditions. Fluctuations in detrital element concentrations were mainly the consequence of wet/arid oscillations. Productivity has been established using Ba excess, according to which marine productivity appears to have been greatest during cold events Heinrich 1 and Younger Dryas. The S1 time interval was not as marked by increases in productivity as was the eastern Mediterranean. In contrast, the S1 interval was first characterized by a decreasing trend and then by a fall in productivity after the 8.2 ky BP dry-cold event. Since then productivity has remained low. Here we report that there was an important redox event in this basin, probably a consequence of the major oceanographic circulation change occurring in the western Mediterranean at 7.7 ky BP. This circulation change led to reventilation as well as to diagenetic remobilization of redox-sensitive elements and organic matter oxidation. Comparisons between our paleoceanographic reconstruction for this basin and those regarding other Mediterranean basins support the hypothesis that across the Mediterranean there were different types of responses to climate forcing mechanism. The Algero–Balearic basin is likely to be a key area for further understanding of the relationships between the North Atlantic and the eastern Mediterranean basins.

Keywords: Western Mediterranean; Balearic basin; Paleoclimate records; Holocene/late glacial

1. Introduction

The Mediterranean has been the focus of intense paleoclimate research. In particular, for North Atlantic circulation, and thus for global climate, mediterranean thermohaline circulation has been of substantial importance (e.g., Johnson, 1997; Sierro et al., 2005). In addition,

* Corresponding author.
E-mail addresses: fjjspejo@ugr.es (F.J. Jimenez-Espejo), fmruiz@ugr.es (F. Martinez-Ruiz), tats-rom@jamstec.go.jp (T. Sakamoto), kiijima@jamstec.go.jp (K. Iijima), haradan@jamstec.go.jp (N. Harada).

0031-0182/$ - see front matter © 2006 Elsevier B.V. All rights reserved.
doi:10.1016/j.palaeo.2006.10.005

the Mediterranean has been especially sensitive to climatic change, such as Dansgaard–Oeschger (D/O) and Monsoonal cycles, Heinrich events (H), etc. A multitude of interdisciplinary approaches have led to an enormous quantity of climate data within different time-frames (e.g., Rossignol-Strick, 1985; Cacho et al., 1999; Emeis et al., 2000a; Krijgsman, 2002; Weldeab et al., 2003; Colmenero et al., 2004; Martrat et al., 2004; Moreno et al., 2005). It is now well-known that in the eastern and western Mediterranean basins climatic responses have been significantly different. The eastern Mediterranean has been characterized by the cyclical deposition of sapropels since the Messinian (e.g., Rossignol-Strick et al., 1982; Rohling and Hilgen, 1991; Emeis and Sakamoto, 1998; Emeis et al., 2000b). Although organic rich-layers have also been reported in the West (Comas et al., 1996), the absence of true sapropels clearly distinguishes both regions. To date, no equivalent of the most recent sapropel from the eastern basin (S1, Mercone et al., 2000) has been reported in the westernmost basin (Martinez-Ruiz et al., 2003). However, it is likely that climatic records from basins located near the limit between the eastern and western basins will make it possible to determine the gradients and differences in climate responses. Because it is situated in the central part of the western Mediterranean, the Algero–Balearic basin is a key location for the understanding of such differences and circulation patterns during the last glacial cycle. This basin is largely isolated from direct continental/river discharge and from tectonic activity, thus providing a unique record for climate-related responses at centennial/millennial scale (Comas et al., 1996).

A multiproxy approach of this record has been performed at ODP Site 975. Regarding circulation, this site enables the monitoring of the history of eastbound inflowing Atlantic waters and westbound outflowing Mediterranean waters (Fig. 1). ODP core 975B-1H was sampled for high-resolution geochemical and mineralogical analyses. Reconstruction of climatic responses have been made by using a number of proxies: Ba and Ba/Al ratios as paleo-productivity proxies (e.g., Dymond et al., 1992; Paytan, 1997) and, U and other redox sensitive elements as proxies for paleo-redox conditions and ventilation processes. Moreover, redox sensitive elements have also provided data regarding post-depositional diagenetic processes. Sedimentary regime conditions have been established based on interpretations of detrital elements and bulk and clay mineralogy.

1.1. Oceanographic setting

At present the western Mediterranean Sea (WMS) dynamic is driven by frontal and turbulent regimes, rather than by thermohaline processes linked to atmospheric seasonality. Eddies thus play a major role in the exchange of water masses (Millot, 1999). The Balearic Channels are important passages for meridional exchanges between the cooler, more saline waters of the northern basins (Gulf of Lion), and the warmer, fresher waters of the southern basins (Alboran and Algero–Balearic basins) (Pinot et al., 2002). Surface water is composed of inflowing Atlantic water progressively modified by air–sea interaction and is referred to in the literature as Modified Atlantic Water (MAW) (Fig. 1). Below the MAW flows the Mediterranean Intermediate Water (MIW) (Cramp and O'Sullivan, 1999). The deepest levels are filled with the Western Mediterranean Deep Water (WMDW), which is formed via deep convection in the Gulf of Lion (Fig. 1) (Benzohra and Millot, 1995). The production of WMDW is controlled by wind strength, initial density of source waters, and the circulation patterns (Pinardi and Masetti, 2000). North-westerlies constitute the major driving force for deep water formation, as well as for enhanced thermohaline circulation (Millot, 1999; Cacho et al., 2000).

Concerning marine productivity, the Mediterranean Sea is an oligotrophic area (Cruzado, 1985). However, one of the highest productivity level is located in the westernmost Mediterranean and is associated with upwelling activity and the hydrological structures of surface waters (Morel, 1991). Organic nutrients are brought to the WMS by Atlantic inflow (Dafner et al., 2001), whereas mineral nutrients are mainly of eolian and fluvial origin, though they sometimes come from deep Mediterranean waters. Eolian input is especially important for Fe, N and other nutrient elements (Gomez, 2003). Phosphate, which is mainly of fluvial origin, is the limiting nutrient for primary production in the Mediterranean Sea (Krom et al., 1991). A physical–biological coupling has been described for the Algero–Balearic southern margin, being that primary production displays a rapid response to the dynamic conditions (Lohrenz et al., 1988; Moran et al., 2001) associated with frontal and eddy circulation.

2. Materials and methods

2.1. Site description

ODP Site 975 is located on the Southern Balearic Margin between the Balearic Promontory (Minorca and Majorca islands) and the Balearic Abyssal Plain (38° 53.795′ N 4° 30.596′ E; 2416 m below sea level, see Fig. 1). Sediments at this site consist of nannofossil or calcareous clay, nannofossil or calcareous silty clay, and

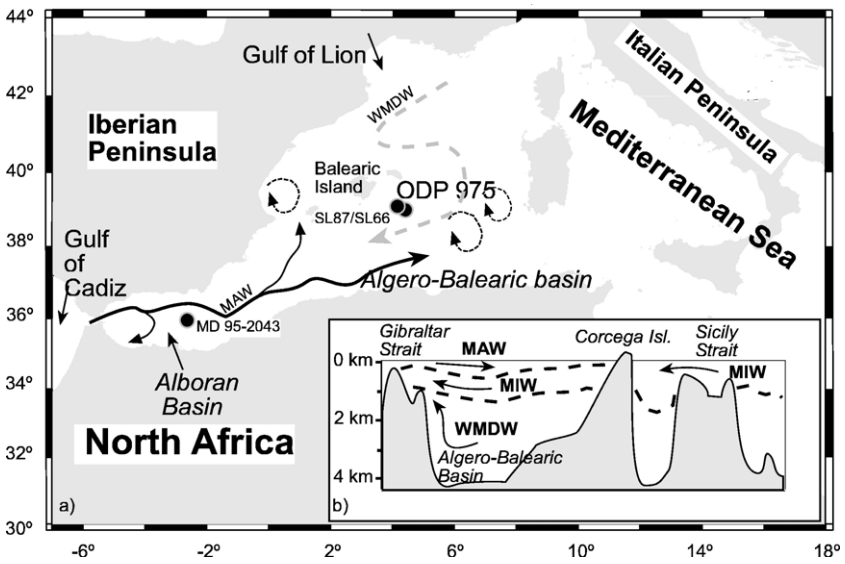

Fig. 1. a) Map of the western Mediterranean showing the location of the studied core, ODP Site 975 and other related cores. West longitudes are negative. Arrows represent the main oceanographic currents. Black line indicates the Modified Atlantic Water (MAW). Dotted lines correspond to eddies. Dashed line represents the Western Mediterranean Deep Water (WMDW). b) Cross section showing main currents (MIW: Mediterranean Intermediate Water). Arrows indicate flow direction. Modified from Cramp and O'Sullivan (1999).

slightly bioturbated nannofossil ooze (Comas et al., 1996). The upper 150 cm of core 975B-1H were sampled continuously every 2 cm. Sediment samples were divided into two portions, one dried and homogenized in agate mortar for mineralogical and geochemical analyses, the other used to separate marine planktonic foraminifers.

2.2. Age model and sedimentation rate

The age model for the sampled interval is based on five ^{14}C-AMS dates (accelerator mass spectrometry) recorded in monospecific planktonic foraminifers (Table 1) (Leibniz-Labor for Radiometric Dating and Isotope Research). The validity of the model is also strengthened by stable isotope stratigraphy and major biostratigraphic variations. In order to compare our data with other paleoclimatic records, all ^{14}C-AMS ages were calibrated to calendar years (cal. BP) using Calib 5.0 software (Stuiver and Reimer, 1993). We used the standard marine correction of 400 yr, as well as the Marine04 calibration curve (Hughen et al., 2004). Linear extrapolation between radiocarbon ages may therefore result in spurious differences in age among time-parallel markers. Thus, we have compared our stable isotopic curve with other paleo-SST records in the WMS, where $\delta^{18}O_{G.\ bulloides}$ fluctuations are synchronous with those of SST at millennial timescale (Cacho et al., 2001).

The linear sedimentation rates (LSR) of late Holocene sediments are 4.4 cm/ky (2050–0 cal. yr BP), approximately half of the older sediments sampled at this location: 7.7 cm/ky at 7500–2050 cal. yr BP, 7.0 cm/ky at 13,250–7500 cal. yr BP and 7.8 cm/ky at 20,000–13,250 cal. yr BP. These LSR values are slightly higher than the ones corresponding to the Algero–Balearic basin (e.g., Martinez-Ruiz et al., 2003; Weldeab et al., 2003).

Table 1
Results of AMS ^{14}C carbon dating of single planktonic foraminifer *G. bulloides* (>125 μm) taken from ODP core 975B-1H

Lab. code	Sample description	Core depth	Conventional age	Calibrated age
KIA 27327	975B/1/8–10, 1.0 mg C	9 cm	2455+30/−25 BP	2049±54 cal BP
KIA 27328	975B/1/50–52, 1.0 mg C	51 cm	7070+40/−35 BP	7519±42 cal BP
KIA 27329	975B/1/90–92, 0.9 mg C	91 cm	13,330±60 BP	15,201±135 cal BP
KIA 27330	975B/1/130–132, 0.8 mg C	131 cm	15,870±80 BP	18,768±67 cal BP
KIA 27331	975B/2/45–47, 1.0 mg C	190 cm	19,460±110 BP	22,512±114 cal BP

Calibration has been made using Calib 5.0 software.
Reservoir effect 400 yr. (One sigma ranges).

They are twice the sedimentation rates estimated for open marine eastern Mediterranean Sea (EMS) ODP sites (Emeis et al., 1996) and five-fold lower than those of the Alboran basin (Comas et al., 1996). Temporal resolution of samples taken from the core is ~400 to 175 yr, which makes it possible to distinguish millennial/centennial climate oscillations.

2.3. Mineralogy

Bulk and clay mineral compositions were obtained by X-ray diffraction (XRD). For bulk mineral analyses, samples were packed in Al sample holders. For clay mineral analyses, the carbonate fraction was removed using acetic acid. The reaction was initiated at a very low acid concentration (0.1 N), and the concentration was increased to 1 N, depending on the carbonate content of each sample. Clay was deflocculated by successive washing with demineralised water after carbonate removal. The <2-μm fraction was separated by centrifugation at 9000 rpm for 1.3 min. The clay fraction was smeared onto glass slides for XRD. Separation of the clay fraction and preparation of samples for XRD analyses were performed following the international recommendations compiled by Kirsch (1991). X-ray diffractograms were obtained using a Philips PW 1710 diffractometer with Cu-Kα radiation and an automatic slit. Scans were run from 2–64° 2θ for bulk-sample diffractograms and untreated clay preparations, and from 2–30° 2θ for glycolated clay-fraction samples. Resulting diffractograms were interpreted using Xpowder software (Martin, 2004). Peak areas have been measured in order to estimate semi-quantitative mineral content. Representative samples were also prepared following the "filtration method" using internal standard (MoS) (Quakernaat, 1970; Iijima et al., 2005). The estimated semiquantitative analysis error for bulk mineral content is 5%; for clay minerals it ranges from 5% to 10%; although semiquantitative analysis aims to show changes or gradients in mineral abundances rather than absolute values.

Morphological studies on selected samples were performed by means of field emission scanning electron microscopy (FESEM), whereas quantitative geochemical microanalyses of the clay minerals were obtained by transmission electron microscopy (TEM) using a Philips CM-20 equipped with an EDAX microanalysis system. Quantitative analyses were obtained in scanning TEM mode only from the edges using a 70-Å diameter beam and a scanning area of 200×1000 Å. In order to avoid alkali loss, a short counting time (30 s) was selected, thus providing better reproducibility for alkali contents (Nieto et al., 1996).

2.4. Geochemical analyses

Total organic carbon (TOC) and total nitrogen content were measured by a CHN analyzer in separate portions of air-dried sediment samples (Perkin Elmer 2400 Series 2). Each powder sample was treated with HCl (12N) in a silver cup, until mineral carbon was completely removed. Samples were then wrapped after dehydration on a hot plate for 12 h. Standards and duplicate analyses were used as controls for the measurements and indicate an error of less than 0.05%.

Major element measurements (Mg, Al, K, Ca, Mn and Fe) were obtained by atomic absorption spectrometry (AAS) (Perkin-Elmer 5100 spectrometer) with an analytic error of 2%. K, Ca, Ti, Mn, Fe, Cu and Sr have also been quantified using an X-Ray Fluorescence scanner (University of Bremen). The XRF-core scanner was set to determine bulk intensities of major elements on split sediment sections (Jansen et al., 1998; Rölh and Abrams, 2000) at intervals of 1 cm with an accuracy in standard powder samples of over 0.20 wt.%. A depth correction was performed to compare AAS and XRF-scanner data. This comparison indicates a high correlation between such techniques. An average for Ti was obtained from XRF-core scanner data in order to normalize Ti to Al contents. This average will be referred to as Ti_{mean}/Al. Analyses of trace elements including Ba were performed using inductively coupled plasma-mass spectrometry (ICP-MS) following HNO3+ HF digestion. Measurements were taken in triplicates by spectrometry (Perkin-Elmer Sciex Elan 5000) using Re and Rh as internal standards. Variation coefficients determined by the dissolution of 10 replicates of powdered samples were higher than 3% and 8% for analyte concentrations of 50 and 5 ppm, respectively (Bea, 1996).

Stable carbon and oxygen isotope ratios of calcareous foraminifers were analysed to establish the stratigraphic framework of core 975B-1H. Approximately 25 specimens of *Globigerina bulloides* were picked from the >125 μm fraction and senescent forms were avoided. Foraminifers were cleaned in an ultrasonic bath to remove fine-fraction contamination, rinsed with distilled water and thoroughly washed in alcohol. Stable isotopes were measured using a GV-Instruments Isoprime mass spectrometer. Analytical reproducibility of the method is ±0.10‰ for both $\delta^{18}O$ and $\delta^{13}C$ based on repeated standards.

2.5. U, Mn, and Fe as redox proxies

Several element/Al ratios have been selected as redox proxies (e.g., Mn/Al, Fe/Al and U/Al). This selection is

based on the fact that manganese and iron oxides are solid phase electron acceptors that are able to reflect paleo-redox conditions. Fe displays a complex redox pattern involving a sequence of burial, dissolution, remobilisation and reprecipitation. Fe content is limited by water column pyrite formation and scavenging, and also by siliciclastic flux and the presence or absence of water column hydrogen sulphide (Lyons et al., 2003). Enrichments in Mn and Fe could be promoted by the diffusion of Mn^{2+} and Fe^{2+} in pore waters from anoxic to oxic layers in which such cations are immobilized. These Fe/Al and Mn/Al enrichments are usually distanced as a result of differences in thermodynamics and kinetic processes (e.g., Thomson et al., 1995; Martinez-Ruiz et al., 2000; Rutten and de Lange, 2003). Patterns in Mn and Fe complement the behaviour of U. When pore water nitrates

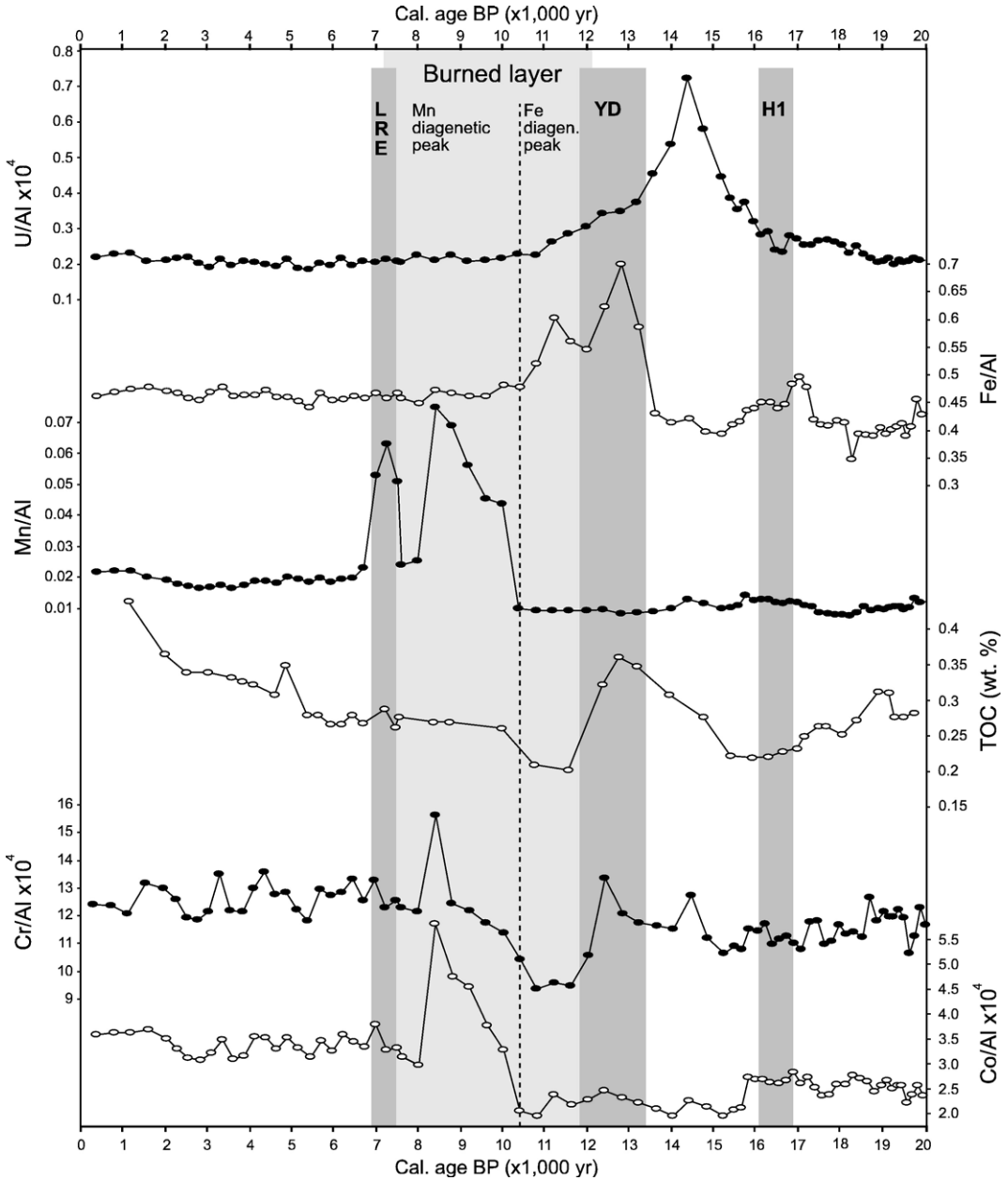

Fig. 2. Total organic carbon wt. (%) (TOC) and elemental/Al ratios according to age plotted as redox proxies. The dark-grey vertical bar indicates the last redox event (LRE) in the Algero–Balearic basin, Younger Dryas (YD) and Heinrich 1 event (H1). Light-grey vertical bar indicates the "burned layer" that evidence re-oxidation processes.

vanish in sediments beneath the redoxcline, U (VI) dissolved in pore water is reduced to immobile U (IV) and precipitates (Anderson, 1982; Barnes and Cochran, 1990; Mangini et al., 2001). In anoxic conditions U becomes immobile, while reduced Mn and Fe can be dissolved in pore water. These oscillations in redox-sensitive element/Al ratios are related to Eh–pH gradients and changes in bottom redox conditions (Mangini et al., 2001). As regards other redox proxies, trace metals display high affinity to Mn and Fe oxi-hydroxides and are common in post-oxic and anoxic pore waters where they are reduced and dissolved. On reaching an oxidative front, these elements can precipitate into other solid phases (Klinkhammer et al., 1982). Organic substances and changes in clay minerals also contribute to this mobilization (Balistrieri and Murray, 1986).

2.6. Ba excess as a productivity proxy in the WMS

Although the use of Ba excess as a proxy has been extensively discussed, recent studies have suggested that it should be applied with greater caution, given that barium requires pore water sulphate concentrations of >15 mM in order to ensure the absence of sulphate reducing sediments (Paytan et al., 1996; McManus et al., 1998a; Eagle et al., 2003), and thus of subsequent barite dissolution or Ba remobilisation (Brumsack, 1986; McManus et al., 1998b). Ba content also depends on sediment provenance, sedimentation rates, Ba cycling within sediments (Mercone et al., 2001; Eagle Gonneea and Paytan, 2006) and lateral transport (Sanchez-Vidal et al., 2005). Another major limitation of the Ba excess signal is that the processes governing its production/accumulation and preservation do not vary over time. Nevertheless, Ba can be considered as a robust proxy for paleoproductivity reconstructions in Mediterranean basins, since Ba, Ba/Al ratios, Ba excess and/or barite accumulation rates have been reliably used by many studies to compare surface productivity changes in the WMS and EMS (e.g., Dehairs et al., 1987; Emeis et al., 2000a; Martinez-Ruiz et al., 2000; Martinez-Ruiz et al., 2003; Weldeab et al., 2003; Paytan et al., 2004), and no indications for barite dissolution have been observed at this site.

3. Results

3.1. Barite and Total Organic Carbon (TOC)

TOC content is under 0.5%, and C_{org}/N ratio values oscillate between 2 and 6, thus suggesting a marine provenance (Meyers, 1994). Depth profiles show a progressive down-core decrease in TOC. Maximum TOC is found in sub-surface samples (0.45%) where organic matter is presently undergoing degradation (Fabres, 2002). Although TOC content shows no major variations along the core, a slight increase followed by a marked drop is observed between the last deglaciation and the Younger Dryas (YD). Minimum TOC content (0.2%) is reached during the Holocene transition (Fig. 2).

FESEM analyses show the presence of barite crystals with morphologies corresponding to typical marine barite (1–5 μm in size with round and elliptical crystals). Detrital elements and Ba peaks display an absence of correlation which also suggests that this barite is of authigenic origin. The Ba content derived from marine barite (Ba excess) has been obtained by subtracting the amount of terrigenous Ba from the total Ba content (e.g., Dymond et al., 1992; Eagle

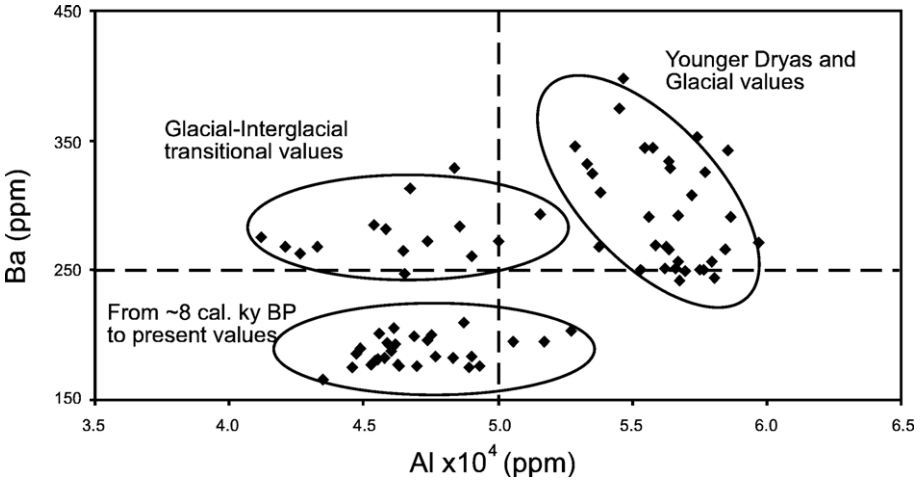

Fig. 3. Ba versus Al (x10^4) content (ppm) in samples from the analyzed time interval.

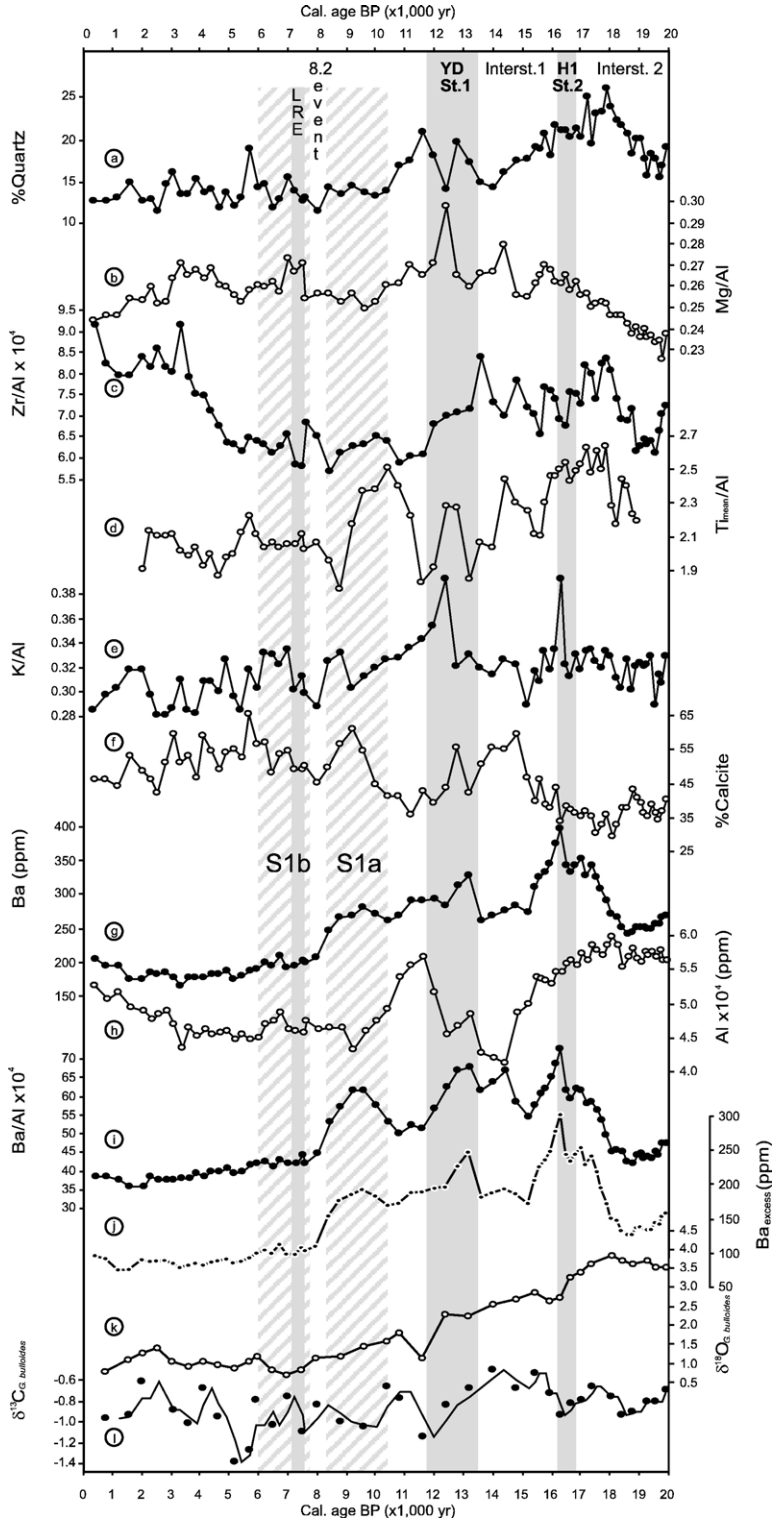

Fig. 4. Core ODP 975B-1H age profiles of: (a) relative quartz concentration (%); (b) Mg/Al ($\times 10^4$) ratio; (c) Zr/Al ($\times 10^4$) ratio; (d) Ti mean/Al ($\times 10^4$) ratio; (e) K/Al ($\times 10^4$) ratio; (f) relative calcite concentration (%); (g) Ba content (ppm); (h) Al content ($\times 10^4$) (ppm); (i) Ba/Al ($\times 10^4$) ratio; (j) Ba excess (ppm); (k) $\delta^{18}O_{G.\ bulloides}$ (‰) and (l) $\delta^{13}C_{G.\ bulloides}$ (‰) 3-period moving average. Ti mean, is an average value obtained from the XRF-scanner. Grey vertical bars indicate the last redox event (LRE) in the Algero–Balearic basin, Younger Dryas (D/O stadial 1) and Heinrich 1 event (D/O stadial 2). Grey-dashed bars represent sapropel S1 (S1a and S1b) time intervals. D/O interstadials and 8.2 cold event are also represented.

et al., 2003). It is used here as the excess associated with crustal phases and is calculated as:

$$(Ba_{excess}) = (total{-}Ba){-}Al(Ba/Al)_{c,}$$

where total-Ba and Al are concentrations and $(Ba/Al)_c$ is the crustal ratio for these elements. In this study, a value of $(Ba/Al)_c = 0.002$ has been used, estimated by Weldeab et al. (2003) for the Balearic Sea on the basis of surface sediments and current oligotrophic conditions. It is assumed that the $(Ba/Al)_c$ ratio of the terrigenous matter remains constant over the period studied. Al is found mainly in aluminosilicates, although it should be kept in mind that this ratio may undergo slight variations. In fact, three regions can be distinguished by comparing Ba and Al content (Fig. 3). A first region of glacial and YD values, (20 to 15 cal. ky BP and 12.3 to 11.1 cal. ky BP), a second region of between 8.2 to 0 cal. ky BP values, and a final region of glacial–interglacial transitional values. This grouping suggests differences in detrital Ba and different $(Ba/Al)_c$ values, although it does not substantially affect the use of Ba_{excess} as a paleoproductivity proxy. On the other hand, the Ba_{excess} enrichment area included the interval between 18.5–18 cal. ky BP and ~8.0 cal. ky BP within which maximum Ba_{excess} content is observed at 16.5–16 cal. ky BP (Fig. 4). Ba_{excess} and TOC do not display similar trends when compared as paleoproductivity proxies. Only one maximum TOC peak during the YD onset coincides with higher values in Ba_{excess}.

3.2. Oxygen and carbon isotope stratigraphy

Variations in $\delta^{18}O_{G.\ bulloides}$ in the WMS support significant climate oscillations since the Last Glacial Maximum. Maximum glacial–interglacial amplitude of $\delta^{18}O_{G.\ bulloides}$ in core 975B-1H lies between 3.84‰ and 0.69‰, with a total oscillation of 3.15‰. The latter value is between that of the Alboran basin (~2.5 ‰) and the Levantine basin located at the EMS (3.5–4‰) (Emeis et al., 2000b). Deglacial warming began between 17.5 and 18 cal. ky BP, displaying thereafter a stable trend (Fig. 4). No major cold reversals have been recognized during the last deglaciation. At the end of the YD and H1 cold events, there were sharp signal decreases that may be representative of short warm periods and/or depleted $\delta^{18}O$ surface currents. After these decrease, $\delta^{18}O_{G.\ bulloides}$ returns to deglaciation warming pattern values. Warming continues into the early Holocene until ~7 cal. ky BP. As of the latter date, the isotopic record displays a cyclical fluctuation pattern whose values are situated between 0.69 ‰ and 1.39 ‰. Values of $\delta^{13}C_{G.\ bulloides}$ were found to be highly variable. The maximum amplitude of $\delta^{13}C_{G.\ bulloides}$ is between −0.5 ‰ and −1.38 ‰, with a total oscillation of 0.88 ‰ $\delta^{13}C_{G.\ bulloides}$ undergoes sudden increase/decrease shifts which do not significantly correlate with the last glacial–interglacial transition.

3.3. Mineralogy and major and trace elements

A complete mineralogical analysis has been performed for a correct interpretation of geochemical data. The sediments sampled at Site 975B are predominantly composed of clay minerals (10–45%), calcite (30–70%) and quartz (10–30%), with low quantities of dolomite and feldspar (<5%). We have also identified accessory minerals, such as zircon, rutile, apatite and biotite, as well as authigenic minerals, such as anhydrite–gypsum, pyrite, Mn and Fe oxi-hydroxides. Clay mineral assemblages consist of illite (50–80%), smectite (20–40%) and kaolinite + chlorite (15%–40%). Additional clay minerals, such as sepiolite, palygorskite and illite/smectite (I/S) mixed layers were also identified using TEM.

Fig. 4 shows the distribution of selected profiles of major and trace element ratios. Elemental concentrations have been normalized to Al. This normalization assumes that Al concentrations in sediments are contributed by alumino-silicates (e.g., Calvert, 1990). High correlation between Al and quartz contents in the analysed interval also corroborates this idea. We detected no grain sorting leading to quartz and heavy mineral enrichments which are associated with turbidites (Wehausen and Brumsack, 1999).

Several element/Al ratios have been used as redox proxies. At the top of the core (<10 cmcd) there is lightly higher in Mn/Al, while a marked double peak can be seen between ~7 to ~10 cal. ky BP (Fig. 2). Before this time, Mn/Al content shows low values within a linear and regular pattern. The most significant Mn/Al enrichment is related to other redox sensitive element/Al ratios, thus indicating the high affinity between these trace metals and Mn oxides. An increase in the Fe/Al ratio consecutively mirrors the double Mn/Al peak. The U/Al ratio displays a linear and regular pattern with one distinct enrichment peak.

4. Discussion

4.1. Sea surface conditions as determined by stable isotopes

Oscillations in $\delta^{18}O_{G.\ bulloides}$ in the WMS are mainly due to changes in SST (Cacho et al., 1999) and to external

fresh water input (Sierro et al., 2005). The first sharp decrease in $\delta^{18}O_{G.\ bulloides}$ was reached around 16 cal. ky BP, and is associated with negative $\delta^{13}C_{G.\ bulloides}$ values and increases in productivity. This pattern of proxies has been attributed to Atlantic currents enriched in iceberg melt waters (Sierro et al., 2005). Nevertheless, according to our age model, the most significant increase in $\delta^{18}O_{G.\ bulloides}$ is located at the end of H1 and could be related to the sharp warming which took place at the end of this cold event (Cacho et al., 2002a). Another sharp increase in $\delta^{18}O_{G.\ bulloides}$ reaching Holocene values occurred at the end of the YD. These warmings arose in Northern Europe later than they did in the areas surrounding the ODP 975B site. They have also been detected around the Iberian margin (Bard et al., 1987) and Mediterranean basins (Cacho et al., 2001), and interpreted in relation to rapid polar front northward movements.

The $\delta^{13}C_{G.\ bulloides}$ values are highly variable (Fig. 4), a fact which could reflect the complexity of the hydrographic processes involved in this region. Changes in $\delta^{13}C_{G.\ bulloides}$ do not follow major climatic/oceanographic oscillations. Decreasing peaks appear during H1 and YD cold events and could be related to a fertilized Atlantic inflow (Rogerson et al., 2004). The lowest $\delta^{13}C_{G.\ bulloides}$ values were attained during the Holocene and could indicate the existence of gyre activities. The latter may have promoted isotopic exchanges with the atmosphere (Broecker and Maier-Reimer, 1992).

4.2. Paleo-redox conditions and diagenetic processes in the Algero–Balearic basin

The Saharan aerosols represent the primary source of Mn in the Algero–Balearic basin (Guieu et al., 1997). Mn distribution within the basin is, however, mainly controlled by bottom-water oxygen conditions (Yarincik et al., 2000). In the uppermost section of core 975B-1H, a slight enrichment in Mn content could be seen as corresponding to current oxic/post oxic limits (Marin and Giresse, 2001; Fabres, 2002). A Mn/Al double peak appears above this enrichment. Minimum TOC values are observed at the lowest Mn double peak boundary coinciding with a relative maximum in the Fe/Al ratio (Fig. 2). This pattern can be accounted for by a redox front promoted by better ventilated deep water covering a sediment which had formed under lower ventilation conditions. Reoxygenation led to hydrogenic deposition or precipitation of the upper Mn/Al peak (Van Santvoort et al., 1996; Thompson et al., 1995). Following this event, an oxidant front began to penetrate downwards through the sediment column. The redox front blocked the upward diffusion of Fe^{2+} and Mn^{2+}, thus forming the lower Mn/Al peak and an upper Fe/Al enrichment (e.g., Rutten et al., 1999). This front is also responsible for an organic matter oxidation, i.e., the "burned layer" (Fig. 2), and for significant alterations in the original uranium content distribution. Sedimentation rate and TOC concentrations control the burn-down depth. According to the model of Jung et al. (1997) a burn-down depth of >20 cm is expected in these conditions (TOC<1% and LSR=5–7 cm/ky). Thus, the latter results fit well with our estimated burn down depth (24 cm), while they also account for the differences between the Ba_{excess} and TOC records.

Similar relationships between Mn, Fe and U have been found in Atlantic (Mangini et al., 2001) and eastern Mediterranean basins and have been interpreted as indicating the penetration of a redox front in which the upper Mn peak represents the uppermost position of the redoxcline (Van Santvoort et al., 1996; De Lange et al., 1999). All of the above-mentioned observations involve the presence of a postdepositional redox front in core 975B-1H. We propose that this last redox event (LRE) was originated by the redoxcline when it reached the ocean floor at 7.5–7.0 cal. ky BP.

4.3. The last redox-event (LRE): paleoceanographic implications

A major oceanographic change, dated at 7.7 cal. ky BP in the Alboran Sea (Perez-Folgado et al., 2003), has been identified from faunal assemblage changes in the WMS. This is related to the progressive increase in Atlantic inflow (Rohling et al., 1995) and consequent deepening of the nutricline and pycnocline (Flores et al., 1997). The LRE recognized in the Algero–Balearic basin has been dated at between 7.5 and 7.0 cal. ky BP and could be linked with this event. Nevertheless, detrital proxies are markedly affected during this event (Fig. 4). These observations suggest scavenging processes and/or synchronous climatic/oceanographic changes. The LRE could represent a recent intensification in thermohaline circulation and/or the first moment in which WMDW fills its deep basins. The cause of these regional variations and the origins of current circulation patterns in the WMS have yet to be clarified. This change may have been caused by variations in surface thermohaline conditions in the WMS which, in turn, are linked with changes in the Atlantic inflow (Rohling et al., 1995) and in the Evaporation/Precipitation ratio (De Rijk et al., 1999; Myers and Rohling, 2000).

4.4. Pre-Holocene productivity in the Algero–Balearic basin

Productivity cannot be described on the basis of the TOC content at Site 975. TOC content was altered by postdepositional oxidation (see Section 4.2), although part of the glacial TOC signal was preserved. The latter signal displays an increase in the vicinity of 15.2 cal. ky BP, which is prior to the deposition of the last organic rich layer (ORL) in the Alboran Sea basin (14.5 to 9.0 cal. ky BP) (Cacho et al., 2002b). Moreover, the Alboran Sea ORL does not coincide with our Ba_{excess} enrichment (~18 to ~8.0 cal. ky BP) and, therefore, no correlation can be observed between the Algero–Balearic basin and the Alboran Sea ORL.

Productivity interpreted on the basis of the Ba_{excess} proxy was highest during the last deglaciation, displaying a maximum peak at 16.5–16 cal. ky BP and a smaller one at the beginning of the YD (Fig. 4). Previous research using core 975B-1H has indicated increases in water productivity during the glacial period and a slight enhancement during sapropel formation in the EMS (e.g., Capotondi and Vigliotti, 1999). Although the highest primary productivity in the Alboran basin was reached during the D/O warm interstadial at 28 to 50 ky (Moreno et al., 2004), at Site 975 we found an inverse signal corresponding to the most recent D/O cycles (Fig. 4). This discrepancy can be explained by the presence of a high isotopic-temperature gradient located between the Morocco and Portugal margins during the YD event and prior to 16 ky. Such a gradient can be accounted for by the presence of the Azores front in the Gulf of Cadiz (Rogerson et al., 2004), which may have created a highly fertilized inflow jet of Atlantic water. It is possible that this jet penetrated into the westernmost WMS basins. Prior to 16 ky, productivity generated by progressive increases in melt water during the last deglaciation could have been further enhanced by this jet inflow. The Azores Front is, however, associated with vigorous upwelling (Alves et al., 2002) and a light $\delta^{13}C_{G.\ bulloides}$ (Rogerson et al., 2004), although the $\delta^{13}C_{G.\ bulloides}$ signal at Site 975 is only slightly affected. The highest Ba_{excess} content during the YD is reached at the beginning of this cold event and may be related to increases in taxa using an r-strategist approach (Young, 1994; Sprovieri et al., 2003). A rise in productivity during the YD has also been recorded at ODP Hole 976C, located in the Alboran basin (Martinez-Ruiz et al., 2004). An eastward displacement of the Alboran gyres and a relatively wet YD have also been proposed as an explanation for increased productivity in the easternmost Alboran basin (Barcena et al., 2001).

4.5. Holocene productivity

At the nearby SL87/KL66 sites, productivity inferred on the basis of biogenic Ba and accumulation rates have been related to glacial (high productivity) and interglacial (low productivity) phases during the late Pleistocene. No increases have been observed in productivity during EMS sapropel deposition (Weldeab et al., 2003). However, in ODP 975B no major decreases in Ba_{excess} occurred at the beginning of the current interglacial period. Early Holocene Ba_{excess} presents values similar to those of the glacial period and the most important decrease in Ba_{excess} took place between 8.5 and 8.0 cal. ky BP. This fall could be related to the faunal change associated with critical increases in Atlantic inflow at 7.7 cal. ky BP (Rohling et al., 1995; Flores et al., 1997) and/or with the 8.2 cal. ky BP cold event reported in other areas of the Mediterranean (e.g., De Rijk et al., 1999; Ariztegui et al., 2000; Sprovieri et al., 2003). The fact that the interval between both events is so short makes it difficult to attribute this fall in productivity to either the earlier or the later event. It is, however, clear that this decrease in Ba_{excess} preceded the LRE, thus indicating that 8.2 may in fact be the most influential event.

The 8.2 cal. ky BP cold event interrupted the deposition of sapropel S1 in the EMS. Wet climate and reduced surface water salinities have been reported in the EMS for the sapropel S1 deposition period (e.g., Combourieu-Nebout et al., 1998; Ariztegui et al., 2000; Myers and Rohling, 2000). The sequences arising from this hiatus have been described as intervals S1a and S1b (Ariztegui et al., 2000). In the WMS, we found high Ba_{excess} values during the period equivalent to the S1a deposition, but low values during S1b. The origin of this divergence is probably linked with the establishment of varying climatic conditions in the WMS and EMS. Following the 8.2 cold event, the EMS returns to wet climatic conditions. In the WMS, however, there is an expansion towards a hot and dry summer Mediterranean climate (Jalut et al., 2000). This may imply a decrease in runoff over all WMS borderlands. Such a marked difference in the climatic conditions affecting both basins, along with the Atlantic/Nile influence, could account for such a large gap in paleoproductivity during S1b deposition between the WMS and EMS.

4.6. Eolian input

At present, the main source of detrital material for the Algero–Balearic basin is the Sahara Desert. Sahara dust is characterized by high quartz, Ti and Zr content (Guieu and Thomas, 1996). In core 975B-1H, Ti_{mean}/Al and Zr/

Al display different degrees of correlation depending on the period in question. The Ti_{mean}/Al signal shows a clear response during the YD, but Zr/Al ratio is not significantly affected by this cold and arid event. Zr/Al values were lowest during the S1 sapropel deposition time interval, thus suggesting humid conditions, whereas a positive peak is observed in Ti_{mean}/Al. These discrepancies in eolian proxies may indicate either a different source area and/or varying sensitivities to wind speed. In particular, we observed that, during the last 5 cal. ky BP, there was a progressive increase in Zr/Al that was perhaps coetaneous to the beginning of the arid period in the Saharan. This most recent rise in Zr/Al is mirrored by the increase in the Ti_{mean}/Al ratio, although to a lesser extent.

On the other hand, palygorskite and fibrous minerals have been related to arid conditions and eolian input in the WMS (Prospero, 1985; Molinaroli, 1996; Foucault and Melieres, 2000). No palygorskite or fibrous clay minerals were detected in core 975B-1H samples which are time equivalent to the S1 sapropel deposition. This also suggests that surrounding margins were influenced by wet conditions and low eolian input. Palygorskite and fibrous minerals (sepiolite, crisotile and kaolinite) are observed following S1 deposition. This suggest enrichment in clay minerals with fibrous morphologies during periods of increased eolian deposition.

4.7. Detrital proxies during the YD

The highest Mg/Al and K/Al ratio values were reached during the YD (Fig. 4). These proxies are associated with fluvial input. The YD is nevertheless considered both a cold and dry period (e.g., Renssen et al., 2001). An intra-YD warm/wet event could promote this high detrital river supply, as long as it is kept in mind that fluvial supply is mainly related to landscape stability and vegetation cover, and not only to increase/decrease in runoff. A strong seasonality during YD (Allen et al., 1996) and/or a significant difference in aridity between northern and southern WMS margins can also contribute to these patterns. Hence, the YD event in the WMS may have developed a particular signal that distinguishes it from other northern hemispheric climatic records.

It is possible that this highest detrital ratio is associated with the short warm event dated at (~12,250 cal. yr BP) and already documented in the Gulf of Cadiz, Alboran Sea and Tyrrhenian Sea (Cacho et al., 2001). In various central European continental records, bi-modal phases have also been reported during YD (Goslar et al., 1993; Walker, 1995; Brauer et al., 2000), whereas there are some southern Iberian Peninsula lake records which do not develop a signal during the YD cold spell (Carrion, 2002).

5. Conclusions

Geochemical and mineralogical proxies show evidence of significant paleoenvironmental changes occurred in the western Mediterranean during the last 20 ky. A redox event (LRE) was established and dated between 7.5 and 7.0 cal. ky BP. This event has deeply influenced both TOC preservation and redox element distribution within these sediments. It has also been related to the beginning of recent frontal circulation in the WMS. Detrital-element profiles also display significant variations which coincide with this LRE. Such variations cannot be accounted for by only increases in Atlantic inflow and would appear to imply scavenging and/or atmospheric changes. Productivity has been characterized by Ba_{excess} and presents fluctuations that can be related to the Atlantic inflow and fresh water input. This productivity was higher during glacial periods and reached its maximums during the YD and ~16 cal. ky BP. A significant productivity decrease started between 8.5 and 8.0 cal. ky BP which has been related to the 8.2 cal. ky BP cold event. Ba profiles support therefore significant productivity differences between the western and eastern Mediterranean at time of S1 sapropel deposition. Thus, comparison of the Algero–Balearic with other Mediterranean basins supports the hypothesis that across the Mediterranean there were different types of responses to climate forcing mechanism. Consequently, this area represents a key location for further understanding of the relationships between the North Atlantic and the eastern Mediterranean basins.

Acknowledgements

We are grateful to the ODP Core Repository personnel (Bremen, Germany) for their assistance with sampling. Analyses were performed at the Analytical Facilities (CIC) and Department of Mineralogy and Petrology (University of Granada), and at the Japanese Agency for Marine–Earth Sciences and Technology (JAMSTEC). The authors are indebted to Dr. K.-C. Emeis for stimulating discussion and to Dr. T. Correge, as editor, and to Dr. N. Fagel and one anonymous reviewer for their invaluable comments and reviews. We are likewise grateful to project CSD2006-00041 and to E. Pinero, E. Abarca, E. Holanda, J. Montes, C. Niembro, D. Ortega for laboratory assistance. Editing of the original English manuscript was done by M. Bettini. This study was financed by Projects REN2003-09130-CO2-01 and CGL2006-13327-C04-04/CLI (MEC), Project RNM432 and Research Group RNM0179 (Junta de Andalucía).

Appendix A. Supplementary data

Supplementary data associated with this article can be found, in the online version, at doi:10.1016/j.palaeo.2006.10.005.

References

Allen, J.R., Huntley, B., Watts, W.A., 1996. The vegetation and climate of north-west Iberia over the last 14,000 yr. J. Quat. Sci. 11, 125–147.

Alves, M., Gaillard, F., Sparrow, M., Knoll, M., Giraud, S., 2002. Circulation patterns and transport of the Azores Front-Current system. Deep-Sea Res. II 49, 3983–4002.

Anderson, R.F., 1982. Concentration, vertical flux, and remineralization of particulate uranium in seawater. Geochim. Cosmochim. Acta 46, 1293–1299.

Ariztegui, D., Asioli, A., Lowe, J.J., Trincardi, F., Vigliotti, L., Tamburini, F., Chondrogianni, C., Accorsi, C.A., Bandini Mazzanti, M., Mercuri, A.M., 2000. Palaeoclimate and the formation of sapropel S1: inferences from Late Quaternary lacustrine and marine sequences in the central Mediterranean region. Palaeogeogr. Palaeoclimatol. Palaeoecol. 158, 215–240.

Balistrieri, L.S., Murray, J.W., 1986. The surface chemistry of sediments from the Panama Basin: the influence of Mn oxides on metal adsorption. Geochim. Cosmochim. Acta 50, 2235–2243.

Barcena, M.A., Cacho, I., Abrantes, F., Sierro, F.J., Grimalt, J.O., Flores, J.A., 2001. Paleoproductivity variations related to climatic conditions in the Alboran Sea (western Mediterranean) during the last glacial–interglacial transition: the diatom record. Palaeogeogr. Palaeoclimatol. Palaeoecol. 167, 337–357.

Bard, E., Arnold, M., Maurice, P., Moyes, J., Duplessy, J.C., 1987. Retreat velocity of the North Atlantic polar front during the last deglaciation determined by $_{14}C$ accelerator mass spectrometry. Nature 328, 791–794.

Barnes, C.E., Cochran, J.K., 1990. Uranium removal in oceanic sediments and the oceanic U balance. Earth Planet. Sci. Lett. 97, 94–101.

Bea, F., 1996. Residence of REE, Y, Th and U in granites and crustal protoliths: implications for the chemistry of crustal melts. J. Petrol. 37, 521–532.

Benzohra, M., Millot, C., 1995. Characteristics and circulation of the surface and intermediate water masses off Algeria. Deep-Sea Res. I 42, 1803–1830.

Brauer, A., Mingram, J., Frank, U., Gunter, C., Georg Schettler, Wulf, S., Zolitschka, B., Negendank, J.F.W., 2000. Abrupt environmental oscillations during the Early Weichselian recorded at Lago Grande di Monticchio, southern Italy. Quat. Int. 73–74, 79–90.

Broecker, W.S., Maier-Reimer, E., 1992. The influence of air and sea exchange on the carbon isotope distribution in the sea. Glob. Biochem. Cycles 6, 315–320.

Brumsack, H.J., 1986. The inorganic geochemistry of Cretaceos black shales (DSDP Leg 41) in compararison to modern upwelling sediments from the Gulf of California. In: Shackelton, N.J., Summerhayes, C.P. (Eds.), North Atlantic Paleoceanography: London. Geological Society Special Publication, vol. 21, pp. 447–462.

Cacho, I., Grimalt, J.O., Pelejero, C., Canals, M., Sierro, F.J., Flores, J.A., Shacklenton, N.J., 1999. Dansgaard–Oeschger and Heinrich event imprints in Alboran Sea temperatures. Paleoceanography 14, 698–705.

Cacho, I., Grimalt, J.O., Sierro, F.J., Shackleton, N., Canals, M., 2000. Evidence for enhanced Mediterranean thermohaline circulation during rapid climatic coolings. Earth Planet. Sci. Lett. 183, 417–429.

Cacho, I., Grimalt, J.O., Canals, M., Sbaffi, L., Shackleton, N.J., Schonfeld, J., Zahn, R., 2001. Variability of the western Mediterranean Sea-surface temperature during the last 25,000 years and its connection with the Northern-Hemisphere climatic changes. Paleoceanography 16, 40–52.

Cacho, I., Grimalt, J.O., Canals, M., 2002a. Response of the western Mediterranean Sea to rapid climatic variability during the last 50,000 years: a molecular biomarker approach. J. Mar. Syst. 33–34, 253–272.

Cacho, I., Sierro, F., Shackleton, N.J., Elderfield, H., Grimalt, J., 2002b. Reconstructing Alboran Sea hydrography during the last organic rich layer formation. Geochim. Cosmochim. Acta 66, A115.

Calvert, S.E., 1990. Geochemistry and origin of the Holocene sapropel in the Black Sea. In: Ittekkot, V., Kempe, S., Michaelis, W., Spitzy, A. (Eds.), Facets of Modern Biogeochemistry. Springer-Verlag, Berlin, pp. 326–352.

Capotondi, L., Vigliotti, L., 1999. Magnetic and microfaunal characterization of Late Quaternary sediments from the Western Mediterranean: influences about sapropel formation and paleoceanographic implication. In: Zahn, R., Comas, M.C., Klaus, A. (Eds.), Proceedings of the Ocean Drilling Program, Scientific Results. Ocean Drilling Project, College Station, TX, pp. 505–517.

Carrion, J.S., 2002. Patterns and processes of Late Quaternary environmental change in a montane region of southwestern Europe. Quat. Sci. Rev. 21, 2047–2066.

Colmenero, E., Flores, J.A., Sierro, F.J., Bárcena, M.A., Löwermark, L., Schönfeld, J., Grimalt, J.O., 2004. Ocean surface water response to short-term climate changes revealed by coccolithophores from the Gulf of Cadiz (NE Atlantic) and Alboran Sea (W Mediterranean). Palaeogeogr. Palaeoclimatol. Palaeoecol. 205, 317–336.

Comas, M.C., Zahn, R., Klaus, A., et al., 1996. Proc. ODP Init. Reports, vol. 161. Ocean Drilling Program, College Station, TX.

Combourieu-Nebout, N., Paterne, M., Turon, J.-L., Siani, G., 1998. A high-resolution record of the last deglaciation in the Central Mediterranean Sea: Palaeovegetation and Palaeohydrological evolution. Quat. Sci. Rev. 17, 303–317.

Cramp, A., O'Sullivan, G., 1999. Neogene sapropels in the Mediterranean : a review. Mar. Geol. 153, 11–28.

Cruzado, A., 1985. Chemistry of Mediterranean Waters. In: Margalef, R. (Ed.), Western Mediterranean. Pergamon Press, Oxford, pp. 126–147.

Dafner, E.V., Sempere, R., Bryden, H.L., 2001. Total organic carbon distribution and budget through the Strait of Gibraltar in April 1998. Mar. Chem. 73, 233–252.

De Lange, G.J., Van Santvoort, P.J.M., Langereis, C., Thomson, J., Corselli, C., Michard, A., Rossignol-Strick, M., Paterne, M., Anastasakis, G., 1999. Palaeo-environmental variations in eastern Mediterranean sediments: a multidisciplinary approach in a prehistoric setting. Prog. Oceanogr. 44, 369–386.

De Rijk, S., Hayes, A., Rohling, E.J., 1999. Eastern Mediterranean sapropel S1 interruption: an expression of the onset of climatic deterioration around 7 ka BP. Mar. Geol. 153, 337–343.

Dehairs, F., Lambert, C.E., Chesselet, R., Risler, N., 1987. The biological production of marine suspended barite and the barium cycle in the western Mediterranean Sea. Biogeochemistry 4, 119–139.

Dymond, J., Suess, E., Lyle, M., 1992. Barium in deep sea sediment: a geochemical proxy for paleoproductivity. Paleoceanography 7, 163–181.

Eagle, M., Paytan, A., Arrigo, K., Van Dijken, G., Murray, R., 2003. A comparasion between excess Barium and Barite as indicators or export production. Paleoceanography 18, 21.1–21.13.

Eagle Gonneea, M., Paytan, A., 2006. Phase associations of barium in marine sediments. Mar. Chem. 100, 124–135.

Emeis, K.C., Sakamoto, T., 1998. The sapropel theme of Leg 160. Proc. ODP Sci. Res., vol. 160. Ocean Drilling Program, College Station, TX, pp. 29–36.

Emeis, K.C., Robertson, A.H.F., Ritcher, C., et al., 1996. Proc. ODP Init. Reports, vol. 160. Ocean Drilling Program, College Station, TX.

Emeis, K.C., Sakamoto, T., Wehausen, R., Brumsack, H.J., 2000a. The sapropel record of the eastern Mediterranean Sea-results of ocean drilling program Leg-160. Palaeogeogr. Palaeoclimatol. Palaeoecol. 158, 371–395.

Emeis, K.C., Struck, U., Schulz, H.-M., Rosenberg, R., Bernasconi, S., Erlenkeuser, H., Sakamoto, T., Martinez-Ruiz, F., 2000b. Temperature and salinity variations of Mediterranean Sea surface waters over the last 16,000 years from records of planktonic stable oxygen isotopes and alkenone unsaturation ratios. Palaeogeogr. Palaeoclimatol. Palaeoecol. 158, 259–280.

Fabres, J., 2002. Transferència de material fi i registre ambietal en conques marginals: les conques d'Alboran i de Bransfield. Ph D. Thesis. Univ. Barcelona, Spain.

Flores, J.A., Sierro, F.J., Frances, G., Vazquez, A., Zamarreno, I., 1997. The last 100,000 years in the western Mediterranean: sea surface water and frontal dynamics as revealed by coccolithophores. Mar. Micropaleontol. 29, 351–366.

Foucault, A., Melieres, F., 2000. Paleoclimatic cyclicity in central Mediterranean Pliocene sediments: the mineralogical signal. Palaeogeogr. Palaeoclimatol. Palaeoecol. 158, 311–323.

Gomez, F., 2003. The role of the exchanges through the Strait of Gibraltar on the budget of elements in the western Mediterranean Sea: consequences of human-induced modifications. Mar. Pollut. Bull. 46, 685–694.

Goslar, T., Kuc, T., Ralska-Jasiewiczowa, M., Rozanski, K., Arnold, M., Bard, E., Van Geel, B., Pazdur, M., Szeroczynska, K., Wicik, B., Wieckowski, K., Walanus, A., 1993. High-resolution lacustrine record of the late glacial/Holocene transition in central Europe. Quat. Sci. Rev. 12, 287–294.

Guieu, C., Thomas, A., 1996. Saharan aerosol: from the soil to the ocean. In: Guerzoni, S., Chester, R. (Eds.), The Impact of Desert Dust Across the Mediterranean. Kluwer Acad. Publisher, pp. 207–216.

Guieu, C., Chester, R., Nimmo, M., Martin, J.M., Guerzoni, S., Nicolas, E., Mateu, J., Keyse, S., 1997. Atmospheric input of dissolved and particulate metals to the northwestern Mediterranean. Deep-Sea Res. II 44, 655–674.

Hughen, K., Baillie, M., Bard, E., Bayliss, A., Beck, J., Bertrand, C., Blackwell, P., Buck, C., Burr, G., Cutler, K., Damon, P., Edwards, R., Fairbanks, R., Friedrich, M., Guildenson, T., Kromer, B., McCormac, F., Manning, S., Bronk Ramsey, C., Reimer, P., Reimer, R., Remmele, S., Southon, J., Stuiver, M., Talamo, S., Taylor, F., van der Plicht, J., Weyhenmeyer, C., 2004. Marine04 Marine radiocarbon age calibration, 26–0 ka BP. Radiocarbon 46, 1059–1086.

Iijima, K., Jimenez-Espejo, F.J., Sakamoto, T., 2005. "Filtration method" for semi-quantitative powder X-ray diffraction analysis of clay minerals in marine sediments. Japan Agency for Marine–Earth Science Technology. Frontier Research on Earth Evolution, vol. 2, pp. 1–3.

Jalut, G., Amat, A.E., Bonnet, L., Gauquelin, T., Fontugne, M., 2000. Holocene climatic changes in the western Mediterranean, from south-east France to south-east Spain. Palaeogeogr. Palaeoclimatol. Palaeoecol. 160, 255–290.

Jansen, J.H.F., Van der Gaast, S.J., Koster, B., Vaars, A.J., 1998. CORTEX, a shipboard XRF-scanner for element analyses in split sediment cores. Mar. Geol. 151, 143–153.

Johnson, R.G., 1997. Climate control requires a dam at the Strait of Gibraltar. Eos Trans. AGU 78 (27), 280–281.

Jung, M., Ilmberger, J., Mangini, A., Emeis, K.-C., 1997. Why some Mediterranean sapropels survived burn-down (and others did not). Mar. Geol. 141, 51–60.

Kirsch, H.J., 1991. Illite crystallinity: recommendations on sample preparation, X-ray diffraction settings, and interlaboratory samples. J. Metamorph. Geol. 9, 665–670.

Klinkhammer, G., Heggie, D.T., Graham, D.W., 1982. Metal diagenesis in oxic marine sediments. Earth Planet. Sci. Lett. 61, 211–219.

Krijgsman, W., 2002. The Mediterranean: Mare Nostrum of Earth sciences. Earth Planet. Sci. Lett. 205, 1–12.

Krom, M.D., Brenner, S., Kress, N., Gordon, L.I., 1991. Phosphorus limitation of Primary Productivity in the E.Mediterranean sea. Limnol. Oceanogr. 36, 424–432.

Lohrenz, S.E., Wiesenburg, D.A., DePalma, I.P., Johnson, K.S., Gustafson Jr., D.E., 1988. Interrelationships among primary production, chlorophyll, and environmental conditions in frontal regions of the western Mediterranean Sea. Deep-Sea Res. A 35, 793–810.

Lyons, T.W., Werne, J.P., Hollander, D.J., Murray, R.W., 2003. Contrasting sulfur geochemistry and Fe/Al and Mo/Al ratios across the last oxic-to-anoxic transition in the Cariaco Basin, Venezuela. Chem. Geol. 195, 131–157.

Mangini, A., Jung, M., Laukenmann, S., 2001. What do we learn from peaks of uranium and of manganese in deep sea sediments? Mar. Geol. 177, 63–78.

Marin, B., Giresse, P., 2001. Particulate manganese and iron in recent sediments of the Gulf of Lion continental margin (north-western Mediterranean Sea): deposition and diagenetic process. Mar. Geol. 172, 147–165.

Martin, J.D., 2004. Qualitative and quantitative powder X-ray diffraction analysis. URL: http://www.xpowder.com ISBN: 84-609-1497-6.

Martinez-Ruiz, F., Kastner, M., Paytan, A., Ortega-Huertas, M., Bernasconi, S.M., 2000. Geochemical evidence for enhanced productivity during S1 sapropel deposition in the eastern Mediterranean. Paleoceanography 15, 200–209.

Martinez-Ruiz, F., Paytan, A., Kastner, M., Gonzalez-Donoso, J.M., Linares, D., Bernasconi, S.M., Jimenez-Espejo, F.J., 2003. A comparative study of the geochemical and mineralogical characteristics of the S1 sapropel in the western and eastern Mediterranean. Palaeogeogr. Palaeoclimatol. Palaeoecol. 190, 23–37.

Martinez-Ruiz, F., Gonzalez-Donoso, J.M., Linares, D., Jimenez-Espejo, F.J., Gallego-Torres, D., Romero, O., Paytan, A., 2004. Respuesta de la productividad biológica marina al cambio climático: registro de alta resolución de la cuenca del mar de Alborán. Geotemas 6, 125–128.

Martrat, B., Grimalt, J.O., Lopez-Martinez, C., Cacho, I., Sierro, F.J., Flores, J.A., Zahn, R., Canals, M., Curtis, J.H., Hodell, D.A., 2004. Abrupt temperature changes in the Western Mediterranean over the past 250,000 years. Science 306, 1762–1765.

McManus, J., Berelson, W., Klinkhammer, G., Johnson, K., Coale, K., Anderson, R., Anderson, R., Kumar, N., Burdige, D., Hammond, D., Brumsack, H., 1998a. Geochemistry of barium in marine sediments: Implications for its use as a paleoproxy. Geochim. Cosmochim. Acta 184, 1–15.

McManus, J., Berelson, W.M., Klinkhammer, G.P., Johnson, K.S., Coale, K.H., Anderson, R.F., Kumar, N., Burdige, D.J., Hammond,

D.E., Brumsack, H.J., 1998b. Geochemistry of barium in marine sediments: implications for its use as a paleoproxy. Geochim. Cosmochim. Acta 62, 3453–3473.

Mercone, D., Thomson, J., Croudace, I.W., Siani, G., Paterne, M., Troelstra, S.R., 2000. Duration of S1, the most recent eastern Mediterranean sapropel as indicated by AMS radiocarbon and geochemical evidence. Paleoceanography 15, 336–347.

Mercone, D., Thomson, J., Abu-Zied, R.H., Croudace, I.W., Rohling, E.J., 2001. High-resolution geochemical and micropalaeontological profiling of the most recent eastern Mediterranean sapropel. Mar. Geol. 177, 25–44.

Meyers, P.A., 1994. Preservation of elemental and isotopic source identification of sedimentary organic matter. Chem. Geol. 114, 289–302.

Millot, C., 1999. Circulation in the western Mediterranean Sea. J. Mar. Syst. 20, 423–442.

Molinaroli, E., 1996. Mineralogical characterization of Saharan dust with a view to its final destination in Mediterranean sediments. In: Guerzoni, S., Chester, R. (Eds.), The Impact Desert Dust Across the Mediterranean. Kluwer Academic, Dordrecht, pp. 153–162.

Moran, X.A.G., Taupier-Letage, I., Vazquez-Dominguez, E., Ruiz, S., Arin, L., Raimbault, P., Estrada, M., 2001. Physical–biological coupling in the Algerian Basin (SW Mediterranean): influence of mesoscale instabilities on the biomass and production of phytoplankton and bacterioplankton. Deep-Sea Res. I 48, 405–437.

Moreno, A., Cacho, I., Canals, M., Grimalt, J.O., Sanchez-Vidal, A., 2004. Millennial-scale variability in the productivity signal from the Alboran Sea record, western Mediterranean Sea. Palaeogeogr. Palaeoclimatol. Palaeoecol. 211, 205–219.

Moreno, A., Cacho, I., Canals, M., Grimalt, J.O., Sanchez-Goni, M.F., Shackleton, N., Sierro, F.J., 2005. Links between marine and atmospheric processes oscillating on a millennial time-scale. A multi-proxy study of the last 50,000 yr from the Alboran Sea (Western Mediterranean Sea). Quat. Sci. Rev. 24, 1623–1636.

Morel, A., 1991. Light and marine photosynthesis: a spectral model with geochemical and climatological implications. Prog. Oceanogr. 26, 263–306.

Myers, P.G., Rohling, E.J., 2000. Modeling a 200-yr interruption of the Holocene sapropel S1. Quat. Res. 53, 98–104.

Nieto, F., Ortega-Huertas, M., Peacor, R., Arostegui, J., 1996. Evolution of illites/smectite from early diagenesis through incipient metamorphims in sediments of the Basque–Cantabrian basin. Clays Clay Miner. 44, 304–323.

Paytan, A., 1997.Marine barite, a recorder of oceanic chemistry, productivity, and circulation. Ph D. Thesis, Univ. San Diego, California, USA.

Paytan, A., Kastner, M., Chavez, F.P., 1996. Glacial to Interglacial Fluctuations in Productivity in the Equatorial Pacific as Indicated by Marine Barite. Science 274, 1355–1357.

Paytan, A., Martinez-Ruiz, F., Ivy, A., Eagle, M., Wankel, S.D., 2004. Using sulfur isotopes in barite to elucidate the origin of high organic matter accumulation events in marine sediments. In: Amend, J.P., Edwards, K.J., Lyons, T.W. (Eds.), Sulfur Biogeochemistry: Past and Present. Special paper, vol. 379. Geological Society of America, Boulder Colorado, pp. 151–160.

Perez-Folgado, M., Sierro, F.J., Flores, J.A., Cacho, I., Grimalt, J.O., Zahn, R., Shackleton, N., 2003. Western Mediterranean planktonic foraminifera events and millennial climatic variability during the last 70 kyr. Mar. Micropaleontol. 48, 49–70.

Pinardi, N., Masetti, E., 2000. Variability of the large scale general circulation of the Mediterranean Sea from observations and modelling: a review. Palaeogeogr. Palaeoclimatol. Palaeoecol. 158, 153–173.

Pinot, J.M., Lopez-Jurado, J.L., Riera, M., 2002. The Canales experiment (1996–1998). Interannual, seasonal and mesoscale variability of the circulation in the Balearic Channels. Prog. Oceanogr. 55, 335–370.

Prospero, J.M., 1985. Records of past continental climates in deep-sea sediments. Nature 315, 279–280.

Quakernaat, J., 1970. Direct diffractometric quantitative analysis of synthetic clay mineral mixtures with molibdenite as orientation-indicator. J. Sediment. Petrol. 40, 506–513.

Renssen, H., Isarin, R.F.B., Jacob, D., Podzum, R., Vandenberghe, J., 2001. Simulation of the Younger Dryas climate in Europe using a regional climate model nested in an AGCM: preliminary results. Glob. Planet. Change 30, 41–57.

Rogerson, M., Rohling, E.J., Weaver, P.P.E., Murray, J.W., 2004. The Azores Front since the Last Glacial Maximum. Earth Planet. Sci. Lett. 222, 779–789.

Rohling, E.J., Hilgen, F.J., 1991. The eastern Mediterranean climate at times of sapropel formation: a review. Geol. Mijnb. 70, 253–264.

Rohling, E.J., Den Dulk, M., Pujol, C., Vergnaud-Grazzini, C., 1995. Abrupt hydrographic change in the Alboran Sea (western Mediterranean) around 8000 yrs BP. Deep-Sea Res. I 42, 1609–1619.

Rölh, U., Abrams, L.J., 2000. High-resolution, downhole, and nondestructive core measurements from Sites 999 and 1001 in the Caribean Sea: application to the late Paleocene Thermal Maximum. In: Leckie, R.M., Sigurdsson, H., Acton, G.D., Draper, G. (Eds.), Proc. ODP, Sci. Results, vol. 165. Ocean Drilling Program, College Station, TX, pp. 191–203.

Rossignol-Strick, M., 1985. Mediterranean Quaternary sapropels: an immediate response of the African monsoon to variation of insolation. Palaeogeogr. Palaeoclimatol. Palaeoecol. 49, 237–265.

Rossignol-Strick, M., Nesteroff, W.D., Olive, P., Vergnaud-Grazzini, C., 1982. After the deluge: Mediterranean stagnation and sapropel formation. Nature 295, 105–110.

Rutten, A., de Lange, G.J., 2003. Sequential extraction of iron, manganese and related elements in S1 sapropel sediments, eastern Mediterranean. Palaeogeogr. Palaeoclimatol. Palaeoecol. 190, 79–101.

Rutten, A., de Lange, G.J., Hayes, A., Rohling, E.J., de Jong, A.F.M., Van der Borg, K., 1999. Deposition of sapropel S1 sediments in oxic pelagic and anoxic brine environments in the eastern Mediterranean: differences in diagenesis and preservation. Mar. Geol. 153, 319–335.

Sanchez-Vidal, A., Collier, R.W., Calafat, A., Fabres, J., Canals, M., 2005. Particulate barium fluxes on the continental margin: a study from the Alboran Sea (Western Mediterranean). Mar. Chem. 93, 105–117.

Sierro, F.J., Hodell, D.A., Curtis, J.H., Flores, A.A., Reguera, I., Colmenero-Hidalgo, E., Barcena, M.A., Grimalt, J.O., Cacho, I., Frigola, J., Canals, M., 2005. Impact of iceberg melting on Mediterranean thermohaline circulation during Heinrich events. Paleoceanography 20, A2019. doi:10.1029/2004PA001051.

Sprovieri, F., Pirrone, N., Gardfeldt, K., Sommar, J., 2003. Mercury speciation in the marine boundary layer along a 6000 km cruise path around the Mediterranean Sea. Atmos. Environ. 37, 63–71.

Stuiver, M., Reimer, P.J., 1993. Extended 14C data base and revised CALIB 3.0 14C Age calibration program. Radiocarbon 35, 215–230.

Thomson, J., Higgs, N.C., Wilson, T.R.S., Croudace, I.W., De Lange, G.J., Van Santvoort, P.J.M., 1995. Redistribution and geochemical behaviour of redox-sensitive elements around S1, the most recent eastern Mediterranean sapropel. Geochim. Cosmochim. Acta 59, 3487–3501.

Van Santvoort, P.J.M., de Lange, G.J., Thomson, J., Cussen, H., Wilson, T.R.S., Krom, M.D., Strohle, K., 1996. Active post-depositional oxidation of the most recent sapropel (S1) in sediments of the eastern Mediterranean Sea. Geochim. Cosmochim. Acta 60, 4007–4024.

Walker, M.J.C., 1995. Climatic changes in Europe during the last glacial/interglacial transition. Quat. Int. 28, 63–76.

Wehausen, R., Brumsack, H.-J., 1999. Cyclic variations in the chemical composition of eastern Mediterranean Pliocene sediments: a key for understanding sapropel formation. Mar. Geol. 153, 161–176.

Weldeab, S., Siebel, W., Wehausen, R., Emeis, K.-C., Schmiedl, G., Hemleben, C., 2003. Late Pleistocene sedimentation in the Western Mediterranean Sea: implications for productivity changes and climatic conditions in the catchment areas. Palaeogeogr. Palaeoclimatol. Palaeoecol. 190, 121–137.

Yarincik, K.M., Murray, R.W., Lyons, T.W., Peterson, L.C., Haug, G.H., 2000. Oxygenation history of bottom waters in the Cariaco Basin, Venezuela, over the past 578,000 years: Results from redox-sensitive metals (Mo, V, Mn, and Fe). Paleoceanography 15, 593–604.

Young, J.R., 1994. In: Winter, A., Sissier, W. (Eds.), Functions of Coccoliths. Coccolithophores. Cambridge University Press, Cambridge, pp. 63–82.